THESIS

CHARACTERIZATION OF PEAT SOIL HYDRAULIC CONDUCTIVITY AND ITS DEPENDENCE ON VEGETATION TYPE IN MOUNTAIN WETLANDS

Submitted by

Audrey Crockett

Department of Geosciences

In partial fulfillment of the requirements

For the Degree of Master of Science

Colorado State University

Fort Collins, Colorado

Summer 2015

Master's Committee:

Advisor: Michael Ronayne

David Cooper
William Sanford

ABSTRACT

CHARACTERIZATION OF PEAT SOIL HYDRAULIC CONDUCTIVITY AND ITS DEPENDENCE ON VEGETATION TYPE IN MOUNTAIN WETLANDS

Peat-forming wetlands enhance biodiversity and provide carbon storage in mountain environments. Persistence of these wetlands requires sustained water inflows. Reduced or altered inflows associated with climate change could lower the water table, potentially resulting in peat oxidation and carbon release to the atmosphere, as well as the loss of wetland plant and animal species. An understanding of the hydrology and site hydraulic properties is necessary to manage mountain wetlands and assess their vulnerability to climate change. This study characterized the hydraulic conductivity of wetland peat soils in Rocky Mountain National Park (RMNP). Peat-forming wetlands in RMNP are classified as fens because their main source of water is groundwater.

Fens in RMNP contain a broad range of vegetation. Dominant vegetation type is one factor that may influence peat hydraulic conductivity, so the fens in this study were divided based on dominant vegetation type. The three vegetation classifications used were "large sedge," "small sedge," and "heterogeneous," indicating that the fens were dominated by large sedges (mainly *Carex*); small sedges (*Eleocharis quinqueflora*); or a mixture of woody plants, sedges, and moss; respectively.

In this study, field measurements were combined with a numerical model and parameter estimation scheme to produce estimates of hydraulic conductivity with a high degree of confidence. Single-ring infiltration tests were performed in the field. A numerical model was constructed, and a parameter estimation scheme was used to find the hydraulic conductivity that best reproduced the results of the single-ring infiltration test.

The fens dominated by small sedges have significantly lower hydraulic conductivity than the fens dominated by large sedges or heterogeneous vegetation. Fens which have relatively high hydraulic conductivity (those dominated by large sedges or a heterogeneous mixture of plants) may be especially at risk of draining under changing climate regimes. Small-sedge fens may be more likely to maintain a high water table due to their low hydraulic conductivity.

ACKNOWLEDGEMENTS

Funding for this research was provided by the Warner College of Natural Resources Mini-Grant, and by the Geological Society of America. This research was performed under National Park Service Research Permit #ROMO-2013-SCI-0041. I am deeply grateful to the Warner College, Geological Society of America, and the National Park Service for their support of this research.

I would like to thank my advisor, Michael Ronayne, for the opportunity to study at CSU and for his invaluable guidance, support, and field assistance. Andrea Harbin, Jake McCane, and Bridget Ronayne also provided field assistance, and I'm grateful for their good humor in the face of grueling field work and changeable weather. David Cooper's knowledge of the fens and plant identification was indispensable in selecting field sites and describing vegetation; I am also grateful for his careful review of this thesis. William Sanford also deserves thanks for his review and suggestions. I am grateful to all the members of my graduate committee for encouraging me to carefully consider the scientific issues presented in this thesis and clarify my thoughts and writing. I am grateful for the historical water-level data provided by Derek Schook, William Schweiger, and Mike Britten.

I owe my interest in water to my parents, Michele and Harry Crockett, and to a wide array of friends and family with a passion for the outdoors. To all my "extra parents"—thank you. Finally, I am grateful to Pete Bell, whose love and support has been unwavering.

TABLE OF CONTENTS

CHAPTER 1. INTRODUCTION

Peat-forming wetlands are important for their ability to store carbon, improve water quality by capturing sediment and pollutants, and provide valuable wildlife habitat. Peatlands have long been threatened by cutting, and by drainage for agriculture. Drained peatlands release carbon to the atmosphere as organic-matter-rich sediments become oxidized (Armentano and Menges 1986, Chimner et al. 2002). As a result of its potential to act as a positive feedback mechanism to the global carbon cycle, peat response to global climate change has come under scrutiny in recent years (Gorham 1991, Whittington and Price 2006). Fens, in particular, have been under investigation to determine their response to climate change from a variety of perspectives: their ability to be used as gauges of groundwater recharge (Drexler et al. 2013); their continued ability to act as carbon sinks (Wu and Roulet 2014); and their responses to potential changes in hydrologic cycles (Driver 2010, Whittington and Price 2006).

The peat-forming wetlands of Rocky Mountain National Park (RMNP) are fed mainly by groundwater and are classified as fens. Radiocarbon dating of basal peat from high-elevation fens in RMNP indicates that peat formation began close to 12,000 years ago (Cooper 1990). The formation of peat soils requires a high water table, which produces the anoxic conditions under which microbial activity is limited and organic matter remains partially undecomposed. While peat is compressible and therefore the formation of a thick peat layer can help ensure that peat-forming conditions persist by preventing both flooding and drying of the peat surface, such ability is limited by the thickness of the peat and by the magnitude of the climatic changes (Grootjans et al. 2006). In RMNP, most peats occur in areas where the water table is no more than 30 cm below the soil surface (Cooper 1990). Thus, the range of environmental conditions under which peat can form in RMNP is fairly narrow, and the presence of thick peat soils indicates a period of environmental stability.

Climate change is already affecting the hydrology of Colorado mountains (Clow 2010), potentially altering the timing and magnitude of groundwater recharge that sustains fens. Knowledge of peat hydraulic properties is crucial in order to predict fen response (e.g., future water table position and seasonal dynamics) to changes in hydrologic conditions. However, the difficulty of measuring hydraulic conductivity in peat soils is well-documented. Peat density tends to increase with depth (Ingram 1978), and the upper, least-decomposed layer is frequently much more permeable than the lower layers (Boelter 1969b, Letts et al. 2000). Rycroft et al. (1975b) noted that laboratory methods did not yield the same hydraulic conductivity as field methods. Related findings were reported by Schlotzhauer and Price (1999) for a bog in Quebec; for shallow peat samples, the mean hydraulic conductivity determined in the laboratory was almost 5 times greater than the mean value obtained from field testing. These differences may be due to laboratory artifacts (e.g., leakage down the walls of permeameters or nonrepresentative samples packed into columns) and/or the difficulty of interpreting data collected in the field. Previous researchers have remarked on the difficulty of inserting wells for field methods due to the instability of peat soil, and that the effect of inflow from the upper, uncompressed peat layers masked the contribution from the lower, more compressed layers (Rycroft et al. 1975a, Rycroft et al. 1975b). Surridge et al. (2005) point out that piezometer slug tests are often used to estimate hydraulic conductivity, but that in peat soils, which may be heterogeneous and anisotropic, care should be taken in analyzing such tests. The very rapid water level recovery following baildown or slug input, caused by the presence of high conductivity fibrous material, makes data analysis problematic and may limit the usefulness of slug tests in peat.

Although it is expected that the type of vegetation from which peat is derived might have an effect on its hydraulic properties, little research has been done to support this supposition. Many studies have characterized the vegetation in fens (Driver 2010), or investigated the hydraulic properties of peat, but few have attempted to link the dominant vegetation type with the hydraulic properties of the peat. Boelter (1969a) conducted measurements on samples of moss peat and herbaceous peat, reporting significantly higher hydraulic conductivities for the mossy samples. More recently, Gnatowski et al. (2009) investigated the hydraulic properties of fen peat soils in Poland and categorized samples as moss peat, herbaceous peat, or wooden peat; they found that the saturated hydraulic conductivity of moss peat was higher than that of herbaceous and wooden peat.

1.1 Objectives

The objectives of this study were 1) to develop a reliable field-based method to estimate the hydraulic conductivity of wetland peat soils; 2) to characterize the hydraulic conductivity of peat within RMNP fens dominated by different vegetation types; and 3) to investigate the potential relationship between vegetation type and peat soil hydraulic conductivity.

CHAPTER 2. STUDY AREA DESCRIPTION

Field work was conducted in Rocky Mountain National Park (RMNP), Colorado, USA, during the summer of 2014. Three vegetation types were identified in RMNP fens: large sedges (mainly dominated by *Carex* species); small sedges (mainly dominated by *Eleocharis quinqueflora*); and heterogeneous (mixture of woody plants, sedges, and moss). Two fens were selected to represent each vegetation type, for a total of six fens (Table 2-1).

Fens selected for study were chosen based on their vegetation characteristics, ease of access, and research history. Previous related research has been conducted at all of the sites in Table 2-1. Water table dynamics at Big Meadows, for example, have been extensively studied to support wetland restoration efforts. The influence of water table depth on carbon cycling has been investigated at Big Meadows, Green Mountain Fen, Spring Fen, Circle Fen, and Hells Fen (Chimner and Cooper 2003).

All fens are located west of the Continental Divide in Rocky Mountain National Park (Figure 2-1). Geologically, this area is a glacially carved basin. Major bedrock units are the Precambrian age Silver Plume Granite and biotite schist (Braddock and Cole 1990). Sedimentary material within valleys includes Quaternary alluvium, deposited along stream courses and on alluvial fans, as well as glacial till. Several glaciation events covered the area during the Pleistocene (Meierding 1977). Three fens (Circle Fen, Sphagnum Fen, and Hells Fen) are located in the Kawuneeche valley, a large, north-striking valley. The Colorado River flows along the Kawuneeche valley bottom. The other three fens (Big Meadows, Green Mountain Fen, and Spring Fen) are at higher elevations within the Tonahutu Creek watershed, to the east of Kawuneeche Valley.

2.1 Large sedge fens

Big Meadows is a large (63-ha), relatively flat fen dominated by *C. aquatilis* and *C. utriculata* (Schimelpfenig et al. 2014, Cooper 1990). It is bounded on one side by Tonahutu Creek, and on others by steep slopes consisting of bedrock or glacial moraine. Big Meadows has been the subject of extensive research on water table dynamics and their interaction with wetland functions. The fen was ditched and drained for hay production in the early 1900s; as part of a restoration effort, the ditches were blocked in 1990 (Cooper et al. 1998). Remnant ditches with deeper water still exist in the fen, and in some areas, water is draining from the peat into these channels. Woody vegetation grows near the incised channelized areas. Twenty years after the restoration effort at Big Meadows, soil properties (bulk density, porosity, percent organic matter, and residual water content) have not recovered (Schimelpfenig et al. 2014). Peat at Big Meadows is 30-195 cm thick, with evidence of past disturbance by flooding or deposition of alluvium (Cooper 1990). Basal peat at Big Meadows is over 11,000 years old (Cooper 1990).

Green Mountain Fen is roughly 0.5 ha in area and is dominated by *Carex* species. There is a pond near the middle of the fen, which contains a floating mat of vegetation that varies in size depending on the year. Surface water drains from Green Mountain Fen on the west side, but the peat itself is not channelized. Peat thickness at Green Mountain Fen is similar to that at Big Meadows (1.5 m), with no evidence of natural or anthropogenic disturbance (Cooper 1990, Chimner and Cooper 2003). Basal peat at Green Mountain Fen is nearly 12,000 years old, indicating a long period of favorable climate for peat growth (Cooper 1990).

2.2 Small sedge fens

Hells Fen is a lower-elevation fen (Table 2-1) dominated by *Eleocharis quinqueflora*. It is 1.5 ha in size, and the peat is 1.2 m deep (Chimner and Cooper 2003). The fen slopes gently down to the upper Colorado River, where a seepage face exposes the peat. During the summer months, the fen is a direct source of water to the upper Colorado, providing slow release of retained water to the river. The fen is fed by groundwater discharging from the nearby lateral moraine (Chimner and Cooper 2003).

Spring Fen is a 9.0 ha in area and contains peat which is 1.65 m thick (Chimner and Cooper 2003). It supports a variety of vegetation, grading from a sedge fen to a treed fen and into upland spruce-fir forest along a transect from its southwest side to its northeast side (Johnson 1996). This study focused on the sedge-dominated portion of the fen, in which the dominant vegetation is *Eleocharis quinqueflora* (Chimner and Cooper 2003). The fen is fed mainly by springs emerging on the bottom of the southwestern-facing slopes. Spring Fen also displays hummock-hollow topography; on the tops of the hummocks, large sedges are found, so hummocks were avoided when choosing sampling sites.

2.3 Heterogeneous fens

Sphagnum Fen is a low-elevation fen (Table 2-1) on the Kawuneeche Valley floor, which is supported by spring water discharging from a glacial moraine (Schook et al. 2013). It has a patchy forest overstory, underlain by hummocky topography which supports other woody plants, mosses, and sedges. The forest overstory contains *Picea engelmanii, Salix wolfii,* and *Salix planifolia*. *Tomentypnum nitens* and *Plagionmium ellipticum* mosses dominate the understory. Large peat hummocks are dominated by *Sphagnum* (Schook et al. 2013). Infiltration test sites were chosen to exclude large woody plants, but small woody plants and mosses were included in the test areas.

Circle Fen is 0.8 ha in size. This low-elevation fen contains 0.8 m of peat (Chimner and Cooper 2003). It supports woody plants, mosses, and sedges. Like Hells Fen, Circle Fen is on the west side of the Colorado River within the Kawuneeche Valley. It is fed by groundwater discharging from the Red Creek alluvial fan (Chimner and Cooper 2003). The central fen contains *C. aquatilus* and *C. utriculata*, as well as *Eriophorum angustifolium* (Chimner and Cooper 2003).

Table 2-1: Fen characteristics

Fen Name	Location	Elevation (m amsl)	Vegetation type	Dominant species in measurement area
Big Meadows	N 40.314 W 105.812	2866	Large sedge	*Carex aquatilis*, *Carex utriculata*
Green Mountain Fen	N 40.308 W 105.814	2887		*Carex utriculata*
Hells Fen	N 40.390 W 105.853	2740	Small sedge	*Eleocharis quinqueflora*
Spring Fen	N 40.325 W 105.796	2926		*Eleocharis quinqueflora*
Sphagnum Fen	N 40.392 W 105.847	2754	Heterogeneous	*Picea engelmanii, Salix wolfii*, *Salix planifolia*, *Sphagnum* spp., *Tomentypnum nitens*, *Plagionmium ellipticum*
Circle Fen	N 40.383 W 105.855	2743		*Picea engelmanii*, *Carex* spp., *Salix* spp.

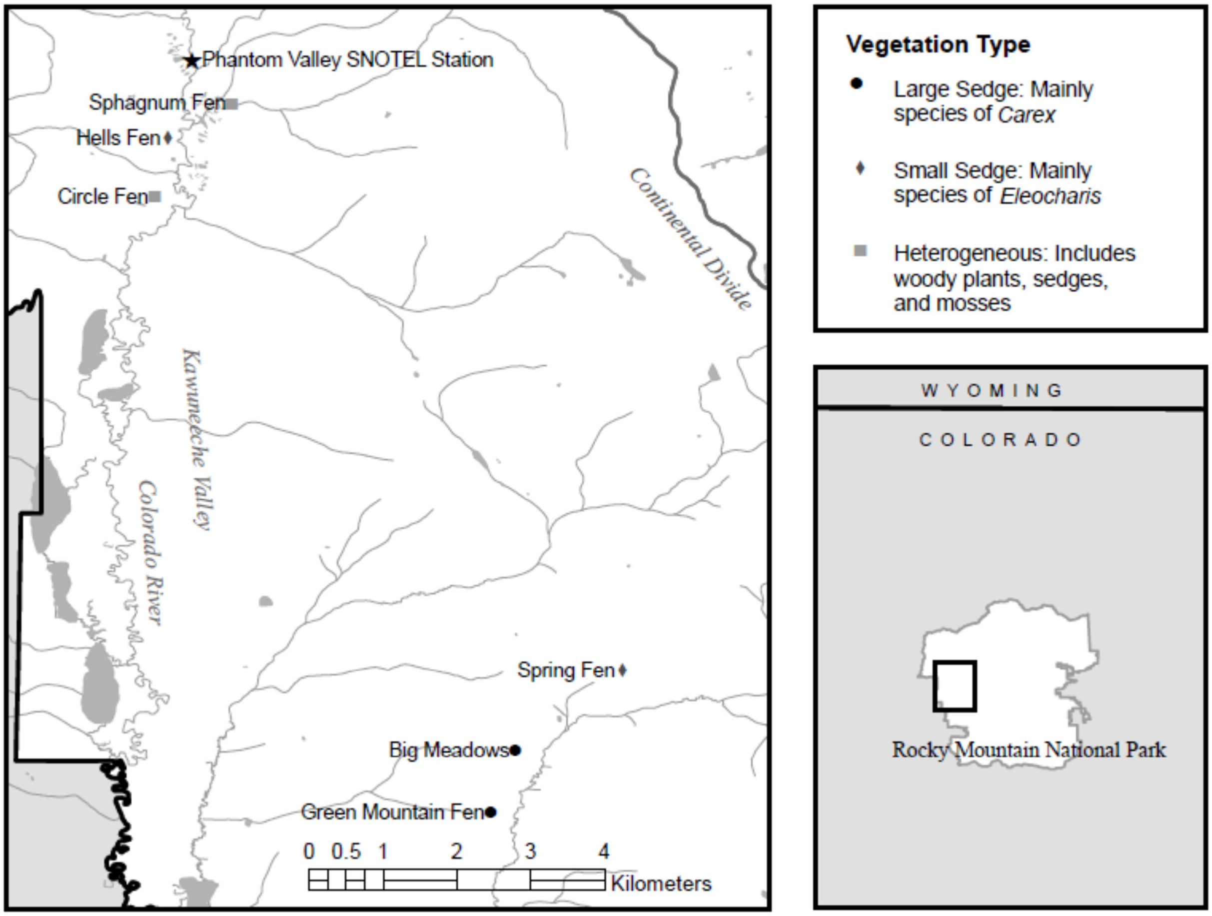

Figure 2-1: Location of fens and study area in Rocky Mountain National Park, Colorado.

CHAPTER 3. METHODS

To produce reliable estimates of saturated hydraulic conductivity, a combination of field testing and computer modeling was used. In the field, ponded infiltration tests were conducted; these measure the steady-state inflow rate at the test site. A numerical model was constructed to simulate the infiltration tests. Saturated hydraulic conductivity was estimated by using a parameter estimation scheme to find the modeled saturated hydraulic conductivity that best reproduced the steady-state inflow rate observed in the field.

3.1 Field methods

Ponded infiltration tests were performed at 4 to 6 locations within each fen to estimate the hydraulic conductivity of the peat. A total of 28 ponded infiltration tests were conducted. Selected test sites were in areas where the characteristic vegetation for each fen (Table 2-1) was well established. Care was taken to avoid disturbing the vegetation and peat soil prior to and during testing.

Field tests were performed using a single-ring infiltrometer, a modification of the more widely-used double-ring infiltrometer method (ASTM 2003). While a double-ring infiltrometer is usually used to satisfy assumptions of strictly vertical flow and unit hydraulic gradient (ASTM 2003), a single-ring method was considered sufficient since three-dimensional flow and a non-unit hydraulic gradient are modeled explicitly under the analysis approach taken in this study.

A steel ring, 30 cm in diameter, was driven into the peat using a hammer. The penetration depth of the ring was between 2 and 4 cm. The ring was filled with water to a known depth, which was generally about 20 cm, and the volume of water added to maintain the applied head was measured over a series of time steps. Volume was measured using a graduated cylinder.

Each test continued until the flow rate through the ring was stable for at least three time steps, which took between 30 and 120 minutes. Figure 3-1 shows example data sets collected at Sphagnum Fen and Hells Fen. The steady-state inflow rate is estimated using inflow volumes during the later part of the test, after the flow field had stabilized. The average steady-state inflow is treated as the measured inflow rate (Q_{meas}) for subsequent modeling analysis and parameter estimation.

Measurement error was estimated based on the precision of the graduated cylinder, and the number of times the cylinder had to be refilled per time step. Measurement error was quantified using

$$M = \frac{1}{n}\sum_{i=1}^{n}\left(\frac{R \times SI}{t}\right), \qquad (1)$$

where *M* is the estimated measurement error in mL/min; *n* is the number of time steps averaged to get the steady-state infiltration value; *R* is the average number of times the graduated cylinder was refilled during the steady-state portion of the test; *SI* is the smallest increment on the graduated cylinder in mL (this depended on the cylinder that was used: for some tests, we used a 2000-mL graduated cylinder with *SI* = 20 mL, while for others we used a 1000-mL graduated cylinder with *SI* = 10 mL); and *t* is the average length of the time steps during the steady-state portion of the test in minutes.

The steady-state inflow rate measured in the infiltration test depends on the effective hydraulic conductivity of the volume sampled. In this type of test, infiltrating water is expected to flow vertically into the soil, then radially out from the ring. Since infiltrated water is expected to flow both vertically and horizontally, the field method does not produce separate estimates of horizontal and vertical hydraulic conductivity. Distinct horizontal and vertical hydraulic conductivity values could exist because of layering of physical and hydraulic properties.

Therefore, the hydraulic conductivity estimated in this study is an effective value across all directions of flow and across a volume, which may contain some heterogeneity.

3.2 Modeling Analysis to Estimate Peat Hydraulic Conductivity

Data from the field tests were analyzed using a numerical groundwater flow model. The two steps involved in the data analysis included (i) setting up a forward model to simulate the infiltration test that was conducted in the field and (ii) performing parameter estimation to identify the peat hydraulic conductivity. The remainder of this chapter provides a detailed description of these modeling activities.

3.2.1 Forward Model

A numerical model of the groundwater flow system was used to account for the three-dimensional flow, non-unit hydraulic gradient, and interfering regional flow system during the infiltration tests. Three-dimensional flow is a result of the high water table at the fens: since the water table was already at the surface, the low hydraulic conductivity of unsaturated soils cannot act as a barrier to prevent horizontal flow, as is the case in traditional infiltration tests, in which an outer ring of water is used to prevent the test water from flowing horizontally. The non-unit hydraulic gradient, again, resulted from the fact that the systems were already saturated when tested: a fairly large head gradient from the top of the ring to the bottom was necessary in order to induce flow. Finally, the fens had already-established regional groundwater head gradients; water tables were near the surface, so shallow groundwater flow is in the direction of the land-surface gradient. This regional flow interacted with the induced head inside the ring to produce the head distributions in the test. All of these issues were accounted for by modeling them explicitly in the numerical flow model.

The model was constructed using the groundwater flow modeling software MODFLOW (Harbaugh et al. 2000), which implements a finite-difference method to solve a three-dimensional groundwater flow equation. Figure 3-2 illustrates the modeling domain and boundary conditions used to simulate infiltration tests conducted in the field. Constant-head boundaries were specified along the left and right edges to model the pre-existing regional hydraulic gradient. The overall domain size (35.81 m × 35.81 m) was chosen such that these external boundaries did not have an effect on ponding-induced head changes near the ring. A gradient of 0.02 was selected based on typical land-surface gradients in the fens, which were derived from a digital elevation model of the park. Since the water table was at or near the surface in all the fens, the land-surface gradient approximated the water-table slope. The total modeled thickness was 5.03 m discretized using 12 layers with thicknesses ranging from 0.02 m (top layer) to 1.68 m (bottom layer). The thickness of the model was chosen so that the model basal contact, which is a no-flow boundary, was located such that it did not influence simulated inflow rates from the ring. While actual peat thicknesses were smaller, if there is leakage from the peat into the underlying glacial sediments, the imposition of a nearer no-flow boundary in the model would have artificially increased estimated hydraulic conductivity rates. The solution provides spatially distributed heads and fluxes (Figure 3-3).

A peat body with greater depth would have increased transmissivity, allowing it to accommodate increased inflow with a lower hydraulic conductivity than might otherwise be necessary. In addition, since the bottom of the model was a no-flow boundary, it was possible that the modeled groundwater flow was interacting with the bottom boundary of the model. In order to test whether the model was sensitive to the depth of the bottom boundary, another model was built with the bottom boundary 2 m lower than the base case, increasing the total model thickness to 7.03 m. The model with the lower bottom boundary was called the low-bottom case. Estimated hydraulic conductivity values for the base case and the low-bottom case agreed to within the estimated 95% confidence intervals for all 28 tests analyzed, indicating that the estimated hydraulic conductivity values are insensitive to the depth of the peat bottom boundary for a reasonable range of depths.

In the vicinity of the infiltration ring, the model grid was refined to a cell size of 2 cm × 2 cm. The ring was modeled as an approximate circle of no-flow cells with an area of 728 cm^2 (Figure 3-2). No-flow cells defining the ring were located in the uppermost layer of the model, which represented the depth to which the ring penetrated the peat during the field tests. The top layer of the model was 2 cm thick, so the modeled penetration of the ring into the subsurface was 2 cm. In order to model the effect of the ponded water, the cells inside the ring were constant-head boundaries. Modeled head inside the ring was adjusted based on the measured water depth inside the ring during each field test, which varied between 18 and 24 cm.

3.2.2 Parameter Estimation

For each infiltration test, parameter estimation was performed to identify the saturated hydraulic conductivity (*K*) value that produces a model-simulated inflow rate which is equal to the inflow rate measured in the field. Hydraulic conductivity was assumed to be constant throughout the model domain, so the problem in question is a one-dimensional (i.e., single parameter), nonlinear regression problem. The relationship between the data and the unknown model parameter, hydraulic conductivity, is given by the numerical MODFLOW model. The following objective function was used to identify the best-fitting *K* value:

$$\min_{K} (Q_{mod} - Q_{meas})^2 \quad (2)$$

where K is the saturated hydraulic conductivity of the peat, Q_{mod} is the modeled steady-steady state infiltration value, and Q_{meas} is the measured steady-state infiltration value for the test in question. The Q_{mod} value was obtained by summing the inflow from all constant-head cells inside the modeled ring extent (Figure 3-3). For each evaluation of Equation 2, the numerical model must be called to produce a value of Q_{meas} using the current estimate of K.

Parameter estimation was performed using Brent's method, an algorithm for inverse parabolic interpolation (Brent 1973). This method does not require calculation of derivatives and is particularly fast for problems in which the objective function is nearly or exactly parabolic, which is the case for the current problem (Figure 3-4).

Using a tolerance of 1×10^{-4}, the algorithm required between 5 and 14 iterations to converge on a best-fit K, with each iteration involving a call of the forward model. The algorithm converges, and the best-fitting K value is identified, when the value of Equation 2 is less than the tolerance. Since each call to the forward model requires rewriting input files and then running MODFLOW, the majority of the computational time rests in the calls to the forward model. For the model setup considered in this study, computing the best-fit saturated hydraulic conductivity for a single infiltration test takes approximately one minute.

Once the best-fit saturated hydraulic conductivity was found for a given test, approximate 95% confidence intervals for the estimated value were calculated. This required the definition of a revised mismatch function, f, that includes measurement error:

$$f(m) = \left(\frac{G(m) - d}{\sigma_{meas}}\right) \tag{3}$$

where $G(m)$ is Q_{mod} (the steady-state inflow rate predicted by the numerical model for the current value of K); d is Q_{meas} (the steady-state inflow rate observed in the ponded infiltration test); m is the model parameter vector (or simply the K value for this single-parameter problem); and σ_{meas} is the standard deviation of the measurement error. The standard deviation of the measurement error, σ_{meas}, was assumed to be equal to the measurement error, *M*, as estimated using Equation 1. In reality, the standard deviation of the measurement errors was likely smaller than this value, so this is a conservative estimate.

Assuming an approximately linear relationship between changes in *f* and changes in the model parameter (*K*), the 95% confidence interval can be estimated as

$$CI_{95} = 1.96 \times \sqrt{\frac{1}{\frac{\partial f(m)}{\partial m} \times \frac{\partial f(m)}{\partial m}}}, \quad (4)$$

which assumes that the model parameter is described by a normal distribution (Aster et al. 2013).

In order to estimate the 95% confidence interval, it is therefore necessary to estimate the gradient of the mismatch function, *f* (Equation 3). A finite-difference approximation was used to do so. The gradient of the objective function around the solution was approximated as

$$\frac{\partial f(m)}{\partial m} \approx \frac{1}{\sigma_{meas}} \left(\frac{G(m+h) - G(m)}{h} \right) \quad (5)$$

where *f(m)* is the value of the objective function at *m*; *m* is the current value of *K*; *G(m)* is the simulated inflow rate Q_{mod} at *m*; and *h* is the step size for the finite-difference approximation. The 95% confidence intervals were insensitive to step sizes between 0.05 and 0.02, indicating that the derivative behavior can be reasonably approximated using this finite-difference method.

Larger confidence intervals are calculated for high-conductivity sites where water moved quickly into the peat, requiring frequent refilling of the 2000-mL graduate cylinder. Example *K* values with 95% confidence intervals are 11.09 ± 0.32 m/day and 0.69 ± 0.03 m/day, respectively, at Sphagnum Fen and Hells Fen, two locations where the peat characteristics are very different.

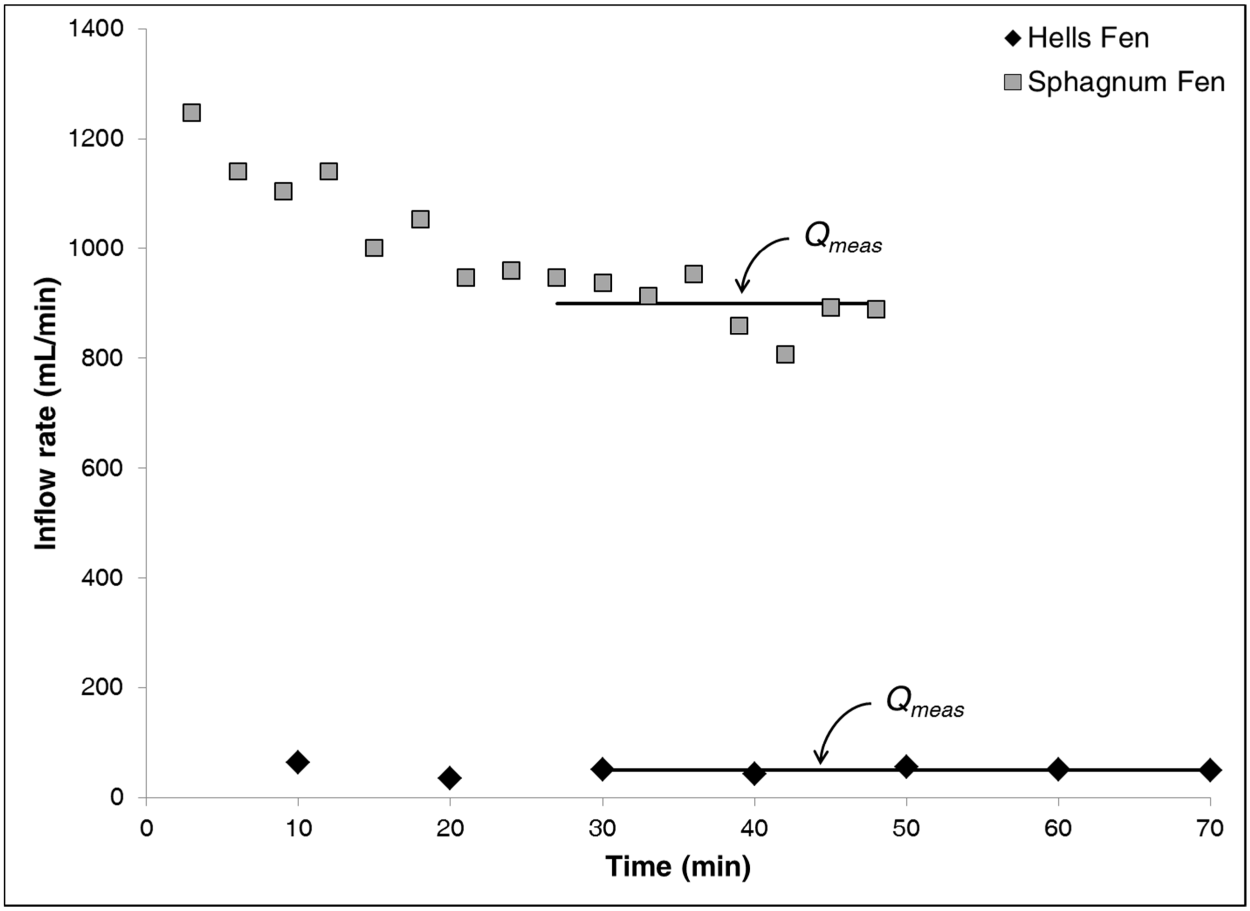

Figure 3-1: Example data for two ponded infiltration tests: a measurement site at Sphagnum Fen with 3-minute time steps and a measurement site at Hells Fen with 10-minute time steps. Posted values (at end of time step) represent the total infiltrated volume during that time step divided by the length of the time step. Horizontal lines labeled Q_{meas} show the estimated steady-state inflow rate.

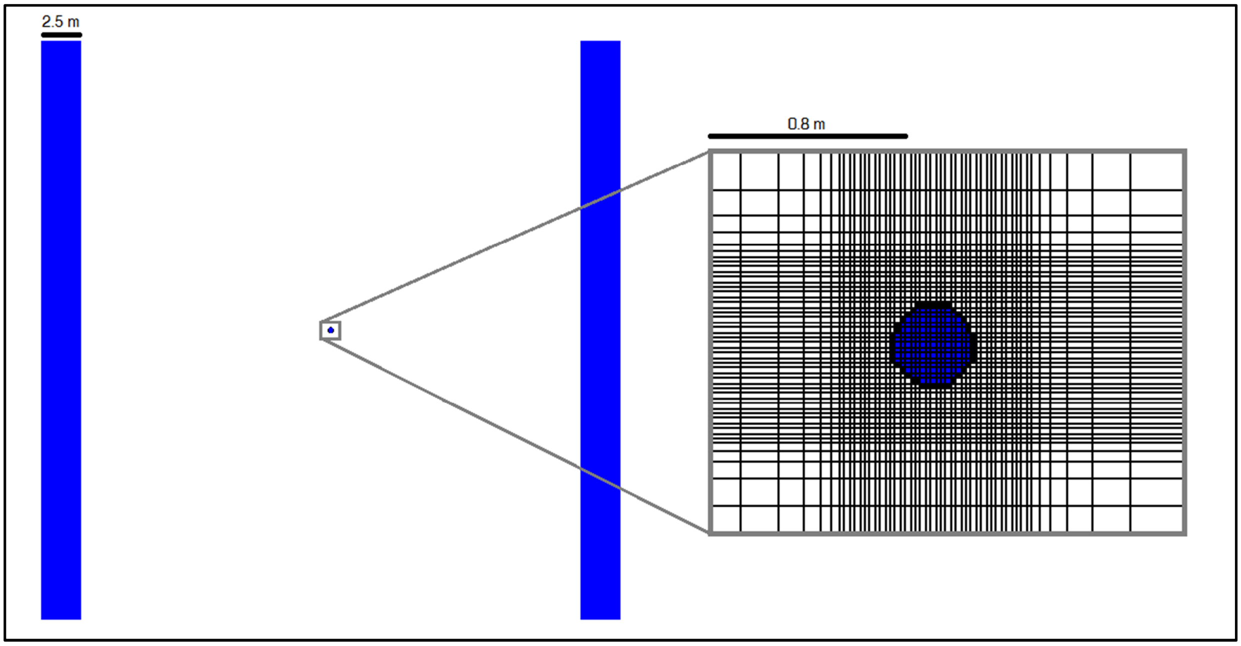

Figure 3-2: Plan view illustration of numerical model domain. Modeled constant-head boundary conditions on the left and right of the domain are shown, and the modeled ring is shown in the middle of the domain. Inset shows finite-difference grid in vicinity of the ring. The steel ring is represented using no-flow cells, whereas model cells inside the ring are assigned a constant-head value based on the depth of ponding established in the field. No-flow cells are shown in black, while constant-head cells are shown in blue.

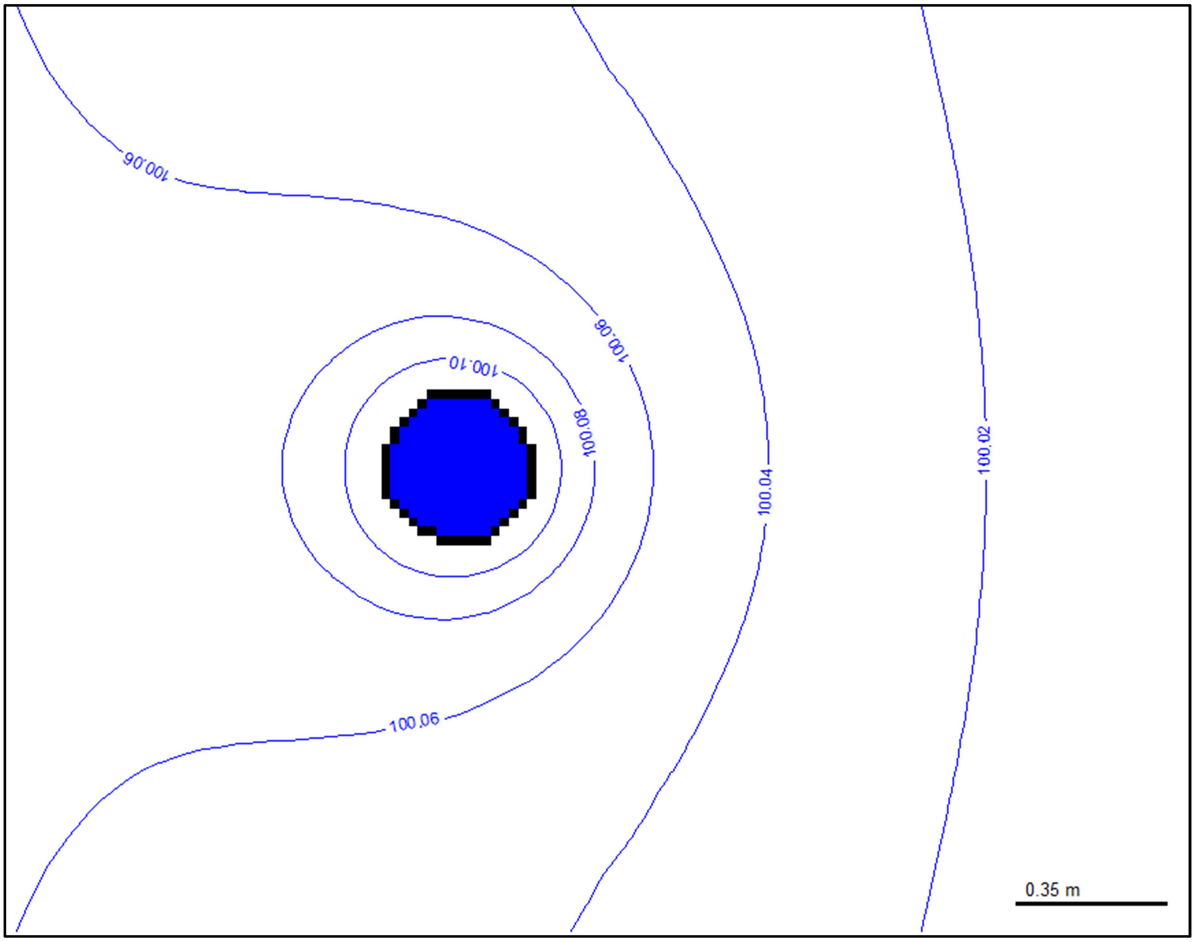

Figure 3-3: Example hydraulic head contours (m) around the ring at the end of a simulated infiltration test. The constant-head value inside the ring was 100.22 m (0.20 m above peat surface) based on conditions established in the field. The simulated head field illustrates the combined effect of left-to-right regional flow and the influence of ponded water inside the ring.

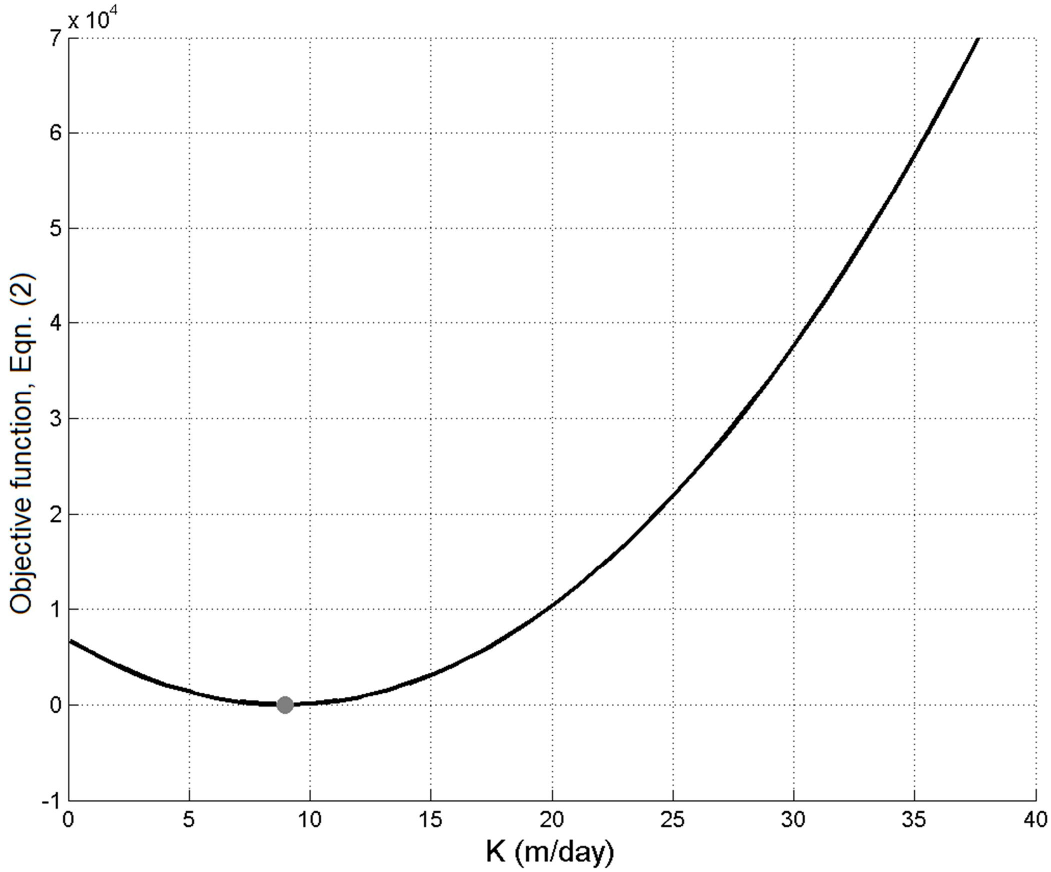

Figure 3-4: Objective function versus hydraulic conductivity (*K*) for infiltration test #6 at Green Mountain Fen. The best-fitting *K* value that minimizes the objective function is 8.96 m/d (shown as the large gray circle).

CHAPTER 4. RESULTS AND DISCUSSION

Results of the field experiments and modeling analyses indicate a wide range of peat soil hydraulic conductivity in RMNP fens. Estimated hydraulic conductivities for all infiltration tests performed are presented in Figure 4-1 and summarized in Table 4-1. The estimated hydraulic conductivity (*K)* values range from 0.4 m/day to 31 m/day. The highest *K* values occurred at the sites with heterogeneous or large-sedge vegetation. The lowest *K* values occurred at the sites with vegetation dominated by *Eleocharis*. The two sites with woody vegetation had the greatest standard deviation in hydraulic conductivity (Table 4-1).

The tight confidence intervals shown with the estimated *K* values reflects the fact that measurement error (associated with field readings of the graduated cylinder) is low compared to the volume of water added during infiltration tests. This is an advantage of the method; stable inflow rates occur and are relatively easy to measure. The points with larger error bars illustrated in Figure 4-1 are from field tests conducted at more permeable sites, where greater volumes of water were used, requiring more frequent refilling of the 2000-mL graduated cylinder. A greater number of refills during a time step means that *R* in Equation 1 is higher, producing a larger estimated error. It is important to note that these confidence intervals are based on the estimated measurement error only. Uncertainty in the conceptual model (i.e., forward modeling assumptions) was not considered when calculating confidence intervals.

Fens with different dominant vegetation types have different hydraulic conductivities. The fens dominated by small sedges have significantly lower saturated hydraulic conductivity than fens dominated by large sedges or woody vegetation (Figure 4-1). The saturated hydraulic conductivity values in the fens dominated by large sedges and those dominated by woody vegetation are not significantly different from each other (Figure 4-1).

The wide range of estimated *K* values is attributed to differences in peat characteristics between fens with different types of vegetation and also to the presence of heterogeneity below the sampling scale. As with all hydraulic tests, the field-based method used in this study gives an effective value of saturated hydraulic conductivity. This effective value is an average of the hydraulic conductivity over a volume of soil that includes some heterogeneity. While the availability of several field tests in each fen provides some insight into heterogeneity at the applied measurement scale, it is impractical to fully characterize the hydraulic conductivity variations at all scales.

4.1 Large sedge fens

The two fens dominated by large sedges (*Carex utriculata* and *Carex aquatilis*) had significantly different saturated hydraulic conductivity values (Figure 4-1). The saturated hydraulic conductivity at Big Meadows was much higher than that at Green Mountain Fen. This may be a result of the differing history of anthropogenic impacts to the two sites. Unlike Big Meadows, Green Mountain Fen has never been impacted by ditching and draining for agriculture.

While restoration efforts at Big Meadows have restored the high water table that sustains wetland conditions (Cooper et al. 1998), the slow rate (~2 cm per century) of peat formation at this site (Cooper 1990) means that the soil properties may not have recovered. Ketcheson and Price (2011) documented an order-of-magnitude difference in peat saturated hydraulic conductivity before and after water table restoration at a bog in Quebec. They attribute this difference to an upper layer of high-*K* peat that was produced by peat expansion on rewetting; such a mechanism may also be affecting the peat at Big Meadows.

Schimelpfenig et al. (2014) measured the saturated hydraulic conductivity of peat samples collected at Big Meadows and obtained lower values (0.5-10 m/day) compared to the estimated hydraulic conductivities from this study. This discrepancy may be the result of differing measurement methods; the previous researchers used soil cores in laboratory constant-head permeameters to measure saturated hydraulic conductivity. Ponded infiltration tests sample a greater area than soil cores, and disturbance by compaction and destruction of the fibrous peat structure is more likely when extracting soil cores.

4.2 Small sedge fens

Fens dominated by small sedges (*Eleocharis quinqueflora*) had the lowest estimated saturated hydraulic conductivity and the smallest standard deviation in saturated hydraulic conductivity compared to the other fen types. The saturated hydraulic conductivity of peat at these fens was significantly different than the saturated hydraulic conductivity of the fens which contained woody vegetation as well as herbaceous vegetation, and from the saturated hydraulic conductivity of Big Meadows. Green Mountain fen did not have significantly different saturated hydraulic conductivity from fens dominated by small sedges.

Fens dominated by small sedges had significantly lower saturated hydraulic conductivity than fens containing heterogeneous vegetation. This may be a result of the type of vegetation from which the peat is derived. Another possible mechanism for this result is that the small sedges are better at capturing fine particles, such as silt, during overland flow events. Finally, it is possible that the hydrologic regime at these sites produces a different rate of decomposition.

This study does not attempt to distinguish the mechanism by which the differences in saturated hydraulic conductivity at the different fens are produced.

4.3 Heterogeneous fens

The fens characterized by a heterogeneous mixture of vegetation had the highest standard deviation in their estimated saturated hydraulic conductivity values (Table 4-1). It is reasonable to expect that this would be the case; these fens contain a variety of vegetation types, including woody plants (*Salix* species and *Picea engelmanii*), sedges, and mosses. Peat derived from diverse vegetation might be expected to be more heterogeneous than peat derived from more homogeneous vegetation.

The two fens in this category, Sphagnum Fen and Circle Fen, had a similar pattern of saturated hydraulic conductivities across multiple measurement sites. Each fen had one measurement site where the saturated hydraulic conductivity was very high, relative to the other infiltration test sites at that fen (Figures 4-1 and 4-2). Soil within these fens may have relatively large channels, formed from the decay or partial decay of buried branches and trunks, surrounded by a peat matrix derived mainly from the herbaceous understory in the fen. Therefore, the high estimated K values may result from the interception of such channels or other heterogeneity in the peat structure.

4.4 Importance for understanding water table dynamics

The peat hydraulic conductivity is an important control on water table dynamics in fens, so these data help explain the hydrograph patterns at each of the sites (Figure 4-3). The relatively constant water table at Hells Fen and Spring Fen may be the result of their low saturated hydraulic conductivity, which enables the fens to release retained water slowly throughout the growing season. Circle Fen demonstrates a response to summer rainfall, as discussed in Chimner and Cooper (2003), which may be the result of its high *K*. Steadily falling water tables at Big Meadows and Green Mountain Fen may reflect their inability to retain water like the lower- *K* sites dominated by *Eleocharis*. Fens characterized by relatively high hydraulic conductivity (fens with large sedges or heterogeneous vegetation) may be especially at risk of draining under changing climate regimes, as their higher saturated hydraulic conductivity makes them less able to retain water and release it slowly throughout a dry period. The low saturated hydraulic conductivity of the fens dominated by small sedges means that they may be able to buffer the effects of a prolonged dry period.

Table 4-1: Mean and standard deviation of estimated hydraulic conductivity values for each fen. Number of ponded infiltration tests at each fen ranged from 4 to 6.

Fen Name	Vegetation type	*K* (m/day)	
		Mean	Standard deviation
Big Meadows	Large sedge	24.42	5.99
Green Mountain Fen		5.79	3.95
Hells Fen	Small sedge	1.05	0.57
Spring Fen		1.93	1.39
Sphagnum Fen	Heterogeneous	13.98	9.18
Circle Fen		11.64	10.06

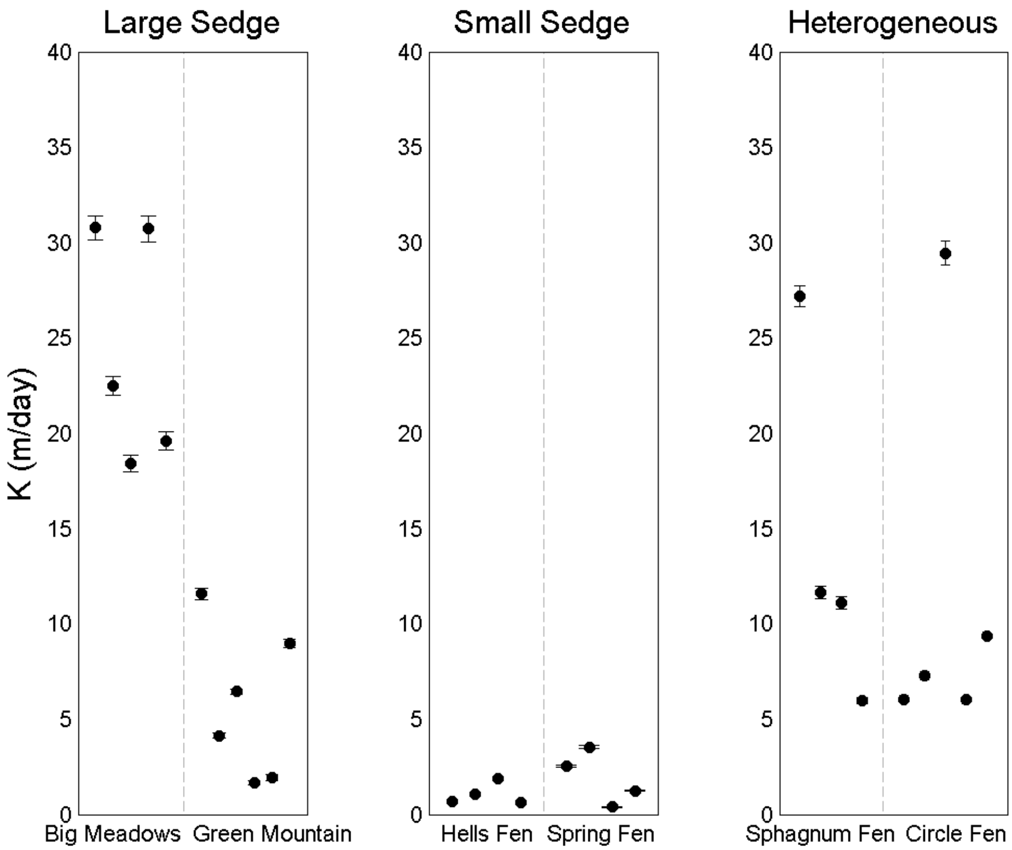

Figure 4-1. Estimated saturated hydraulic conductivity values for 28 ponded infiltration tests. Error bars represent approximate 95% confidence intervals.

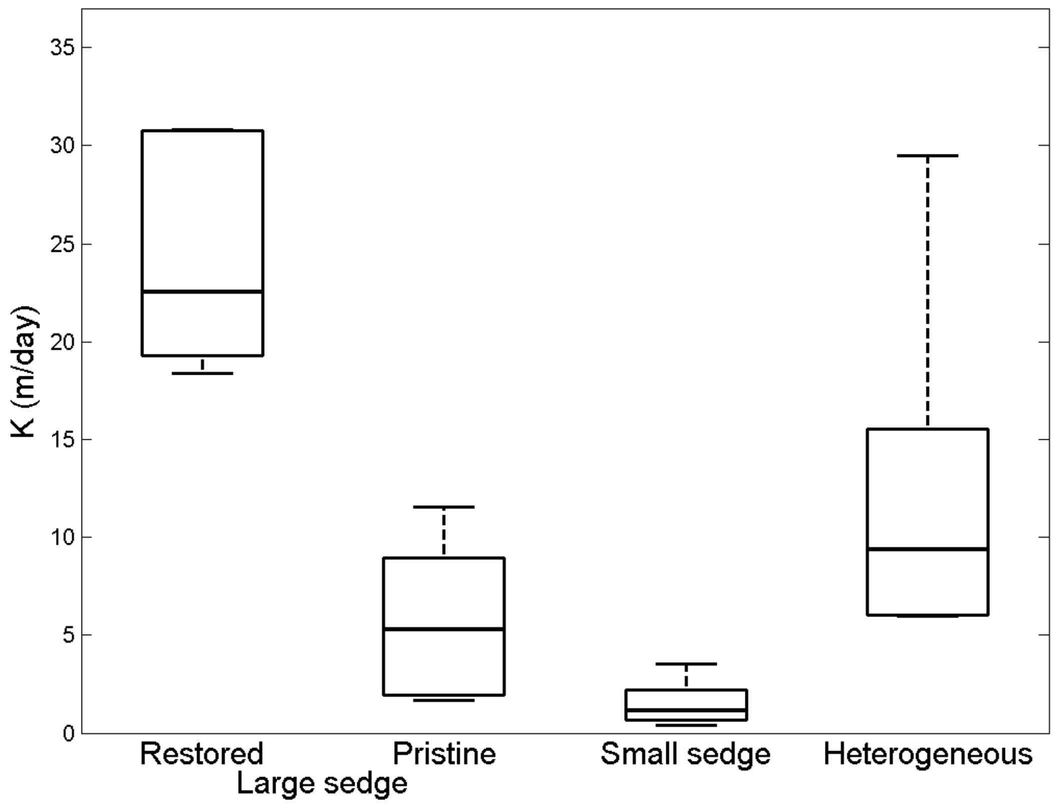

Figure 4-2. Box plots of estimated saturated hydraulic conductivity for the three different vegetation types. Big Meadows and Green Mountain fens are separated to illustrate the potential effects of past site disturbance. Whiskers extend to the minimum and maximum values; the bottom and top of each box represents the 25^{th} and 75th percentile of the data, respectively; and the central mark is the median.

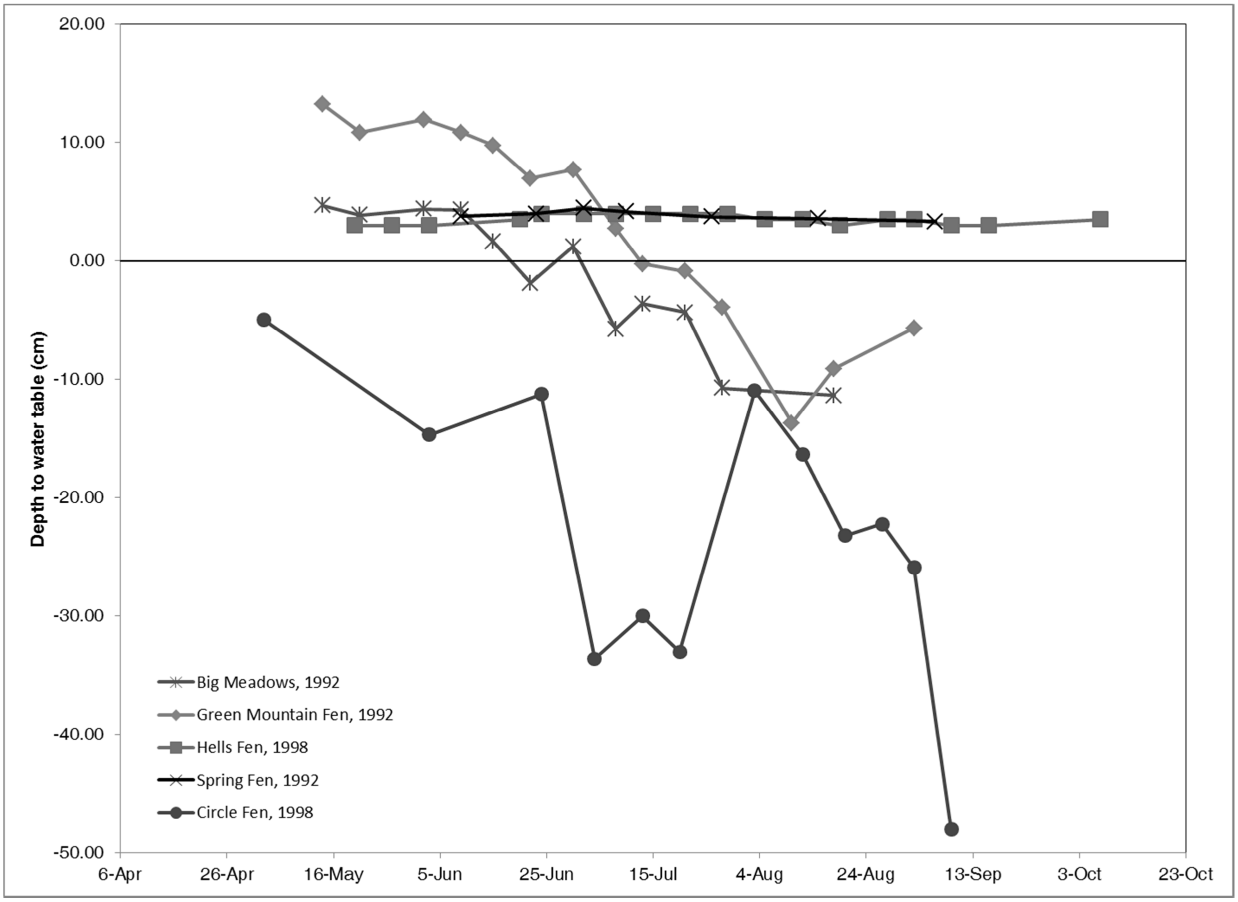

Figure 4-3. Water table depth in five fens through a growing season. Years represented are 1992 and 1998; precipitation patterns were similar in these years. Small sedge fens (Hells Fen and Spring Fen) maintain a nearly constant water table through the growing season, while large sedge fens (Big Meadows and Green Mountain Fen) and the heterogeneous fen (Circle Fen) display falling water tables throughout the summer months. Data are from Schook et al. (2013) and Schweiger (2015).

CHAPTER 5. CONCLUSIONS AND RECOMMENDATIONS

5.1 Summary and Conclusions

This study investigated the relationship between vegetation type and peat soil hydraulic conductivity in RMNP fens. A method was developed to estimate the saturated hydraulic conductivity of peat using data collected during single-ring ponded infiltration tests. Data analysis for each infiltration test involved numerical modeling and parameter estimation to identify the best-fitting saturated hydraulic conductivity value. This field-based method avoids many of the problems encountered during laboratory testing (e.g., representativeness of core samples transported to the laboratory, edge effects and other issues associated with packed columns), and the method may also have advantages over slug testing, particularly for settings with high-conductivity peat where slug-test data are difficult to interpret.

The results of this study demonstrate that the saturated hydraulic conductivity of peat formed in fens differs depending on the dominant vegetation type in the fen. Specifically, fens dominated by the small-sedge species *Eleocharis quinqueflora* are likely to contain peat which has a low hydraulic conductivity. Fens that contain both woody and large-sedge herbaceous vegetation are likely to contain peat characterized by relatively high hydraulic conductivity, and in which the heterogeneity of the hydraulic conductivity field is high as well.

The measured hydraulic conductivities help explain historical water level data, providing a possible mechanism for the differing water table dynamics at the various fens. Fens with high hydraulic conductivity appear to dry more easily than those with low hydraulic conductivity, suggesting that the high- K fens may be more at risk of degradation if the climate becomes drier.

5.2 Recommendations

While the magnitude of a fen's hydraulic conductivity and its vegetation are clearly related, this study does not provide a mechanistic explanation for this relationship. A few mechanisms explaining the hydraulic conductivity-vegetation linkage are plausible. For example, some plants may be better-adapted to survive in a low- or high- *K* environment, so they tend to dominate in such environments. Alternately, if some plants are more likely to cause fine sediments to settle out of overland flow, if such plants dominated a fen, the peat in that fen would have a lower hydraulic conductivity than the peat in nearby fens not dominated by such plants. It is likely that the true explanation is not as clear-cut as either of these examples. Answering the question of whether vegetation tends to cause changes in hydraulic conductivity, or the other way around, could have important implications for fen restoration and for park managers, who may wish to promote the growth of certain types of plants.

The hydraulic testing method described here identifies a single effective hydraulic conductivity, which is influenced by the internal peat structure as well as the geometry of the induced flow system. Layering of physical and hydraulic properties has been observed in many peats. For example, compression and increased decomposition of older peat can produce lower hydraulic conductivities at greater depths (Ingram 1978). Such layering, which could produce distinct horizontal and vertical K values (anisotropic hydraulic conductivity), was not considered in this study. Beckwith et al. (2003) found that anisotropy has the potential to alter the pattern of groundwater flow in a bog peat. Future work involving a more detailed analysis method that explicitly considers layering and anisotropy in fen peats may produce more reliable estimates of the pattern of groundwater flow in fens.

Fens dominated by large sedges will need to be investigated further; no clear pattern to explain their saturated hydraulic conductivity has emerged. This study is hampered by having only two fens to represent each vegetation type. It is recommended that more fens dominated by large sedges be investigated in order to determine whether the large values of saturated hydraulic conductivity that were measured at Big Meadows are anomalous, or representative of other large-sedge fens with prior anthropogenic disturbance.

The fens investigated in this study are in the upper Colorado River watershed near the river's headwaters. All of these fens appear to offer an important water storage function, providing slow release of water throughout the summer dry season. Future work should focus on the interaction of peat-forming fens with the hydrologic regime to determine which fens are most vulnerable to a changing climate and which are most important in terms of ecosystem functions.

BIBLIOGRAPHY

Aguilera, H., S. Castaño, L. Moreno, M. E. Jiménez-Hernández, and A. de la Losa. "Model of the hydrological behaviour of the anthropized semiarid wetland of Las Tablas de Daimiel National Park (Spain) based on surface water-groundwater interactions." *Hydrogeology Journal* 21 (2013): 623-641.

Armentano, T. V., and E. S. Menges. "Patterns of Change in the Carbon Balance of Organic Soil-Wetlands of the Temperate Zone." *Journal of Ecology* 74, no. 3 (1986): 755-774.

Aster, R. C., B. Borchers, and C. H. Thurber. *Parameter Estimation and Inverse Problems.* Second. Waltham, MA: Academic Press-Elsevier, 2013.

ASTM Standard D3385. "Standard Test Method for Infiltration Rate of Soils in Field Using Double-Ring Infiltrometer." *Annual Book of ASTM Standards* 04.08 (2003): 368-374.

Baird, A. J. "Field estimation of macropore functioning and surface hydraulic conductivity in a fen peat." *Hydrological Processes* 11, no. 3 (1997): 287-295.

Beckwith, C. W., A. J. Baird, and A. L. Heathwaite. "Anisotropy and depth-related heterogeneity of hydraulic conductivity in a bog peat. II: modelling the effects on groundwater flow." *Hydrological Processes* 17 (2003): 103-113.

Boelter, D. H. "Important physical properties of peat materials." *Proceedings of the Third International Peat Conference, Quebec, Canada* (1969a).

Boelter, D. H. "Physical Properties of peats as related to degree of decomposition." *Soil Science Society of America Journal* (1969b).

Boeye, D., and R.F. Verheyen. "The hydrological balance of a groundwater discharge fen." *Journal of Hydrology* 137, no. 1 (1992): 149-163.

Braddock, W. A. and J. C. Cole. “Geologic map of Rocky Mountain National Park and vicinity, Colorado,” I-1973 [map]. 1:50,000. Miscellaneous Investigations Series. U. S. Geological Survey (1990).

Brent, R. P. *Algorithms for Minimization without Derivatives.* Englewood Cliffs, N.J. Prentice-Hall, 1973.

Chimner, R. A., and D. J. Cooper. "Carbon dynamics of pristine and hydrologically modified fens in the southern Rocky Mountains." *Canadian Journal of Botany* 81, no. 5 (2003): 477-491.

Chimner, R. A., D. J. Cooper, and W. J. Parton. "Modeling carbon accumulation in Rocky Mountain fens." *Wetlands* 22, no. 1 (2002): 100-110.

Chimner, R. A. *Carbon Dynamics of Southern Rocky Mountain Fens.* Dissertation, Fort Collins, CO: Colorado State University, 2000.

Clow, D. W. "Changes in the timing of snowmelt and streamflow in Colorado: A response to recent warming." *Journal of Climate* 23, no. 1 (2010): 2293-2306.

Cooper, D. J. "Ecology of wetlands in Big Meadows, Rocky Mountain National Park, Colorado." Biological Report, Fish and Wildlife Service, United States Department of the Interior, 1990.

Cooper, D. J., L. H. MacDonald, S. K. Wenger, and S. W. Woods. "Hydrologic restoration of a fen in Rocky Mountain National Park, Colorado, USA." *Wetlands* 18, no. 3 (1998): 335-345.

Dane, J. H. "Comparison of field and laboratory determined hydraulic conductivity values." *Soil Science Society of America Journal* 44, no. 2 (1980): 228-231.

Drexler, J. Z., D. Knifong, J. Tuil, L. E. Flint, and A. L. Flint. "Fens as whole-ecosystem gauges of groundwater recharge under climate change." *Journal of Hydrology* 481 (2013): 22-34.

Driver, K. M. "Distinguishing the hydrologic regimes and vegetation of fens and wet meadows in the Rocky Mountains." Master's thesis, Colorado State University, 2010.

Gilvear, D. J., P. J. K. Sadler, J. H. Tellam, and J. W. Lloyd. "Surface water processes and groundwater glow within a hydrologically complex floodplain wetland, Norfolk Broads, U.K." *Hydrology and Earth System Sciences* 1 (1997): 115-135.

Gnatowski, T., J. Szatyłowicz, T. Brandyk, and C. Kechavarzi. "Hydraulic properties of fen peat soils in Poland." *Geoderma* (2009).

Gorham, E. "Northern peatlands: Role in the carbon cycle and probable responses to climatic warming." *Ecological Applications* 1, no. 2 (1991): 182-195.

Grootjans, A. P., E. B. Adema, W. Bleuten, H. Joosten, M. Madaras, and M. Janáková. "Hydrological landscape settings of base-rich fen mires and fen meadows: An overview." *Applied Vegetation Science* 9 (2006): 175-184.

Harbaugh, A.W., E.R. Banta, M. C. Hill, and M. G. McDonald. "MODFLOW-2000, The U. S. Geological Survey Modular Ground-Water Model – User Guide to Modularization Concepts and the Ground-Water Flow Process." U. S. Geological Survey Open-File Report 00-92, 2000.

Holden, J., and T. P. Burt. "Runoff production in blanket peat covered catchments." *Water Resources Research* 39, no. 7 (2003).

Ingram, H. A. P. "Soil layers in mires: Function and terminology." *Journal of Soil Science* 29, no. 2 (1978): 224-227.

Johnson, J. B. "Phytosociology and gradient analysis of a subalpine treed fen in Rocky Mountain National Park, Colorado." *Canadian Journal of Botany* 74 (1996): 1203-1218.

Ketcheson, S. J., and J. S. Price. "The impact of peatland restoration on the site hydrology of an abandoned block-cut bog." *Wetlands* 31, no. 6 (2011): 1263-1274.

Kværner, J., and B. Kløve. "Generation and regulation of summer runoff in a boreal flat fen ." *Journal of Hydrology* 360, no. 1 (2008): 15-30.

Letts, M. G., N. T. Roulet, N. T. Comer, M. R. Skarupa, and D. L. Verseghy. "Parametrization of peatland hydraulic properties for the Canadian Land Surface Scheme." *Atmosphere-Ocean* 38, no. 1 (2000): 141-160.

Meierding, T. C. "Age differentiation of till and gravel deposits in the Upper Colorado River Basin." PhD thesis, University of Colorado, Boulder, 1977.

Price, J. S., and S. M. Schlotzhauer. "Importance of shrinkage and compression in determining water storage changes in peat: The case of a mined peatland." *Hydrological Processes* 13 (1999): 2591-2601.

Quinton, W. L., M. Hayashi, and A. Pietroniro. "Connectivity and storage functions of channel fens and flat bogs in northern basins." *Hydrological Processes* 17, no. 18 (2003): 3665-3684.

Rycroft, D. W., D. J. A. Williams, and H. A. P. Ingram. "The transmission of water through peat: I. Review." *Journal of Ecology* 63, no. 2 (1975a): 535-556.

Rycroft, D. W., D. J. A. Williams, and H. A. P. Ingram. "The transmission of water through peat: II. Field experiments." *Journal of Ecology* 63, no. 2 (1975b): 557-568.

Schimelpfenig, D. W. "The effects of long term drainage and restoration on soil properties of southern Rocky Mountain sedge fens." Master's thesis, Colorado State University, 2012.

Schimelpfenig, D. W., D. J. Cooper, and R. A. Chimner. "Effectiveness of ditch blockage for restoring hydrologic and soil processes in mountain peatlands." *Restoration Ecology* 22

(2014): 257-265.

Schlotzhauer, S. M., and J. S. Price. "Soil water flow dynamics in a managed cutover peat field, Quebec: Field and laboratory investigations." *Water Resources Research* 35, no. 12 (1999): 3675-3683.

Schook, D., D. J. Cooper, and W. Schweiger. "Relationship of fen vegetation to long-term hydrologic processes in Rocky Mountain National Park, Colorado." Tech. rep., U.S. National Park Service, Rocky Mountain National Park, 2013.

Schweiger, E.W. National Park Service Rocky Mountain Network. Personal communication, 2015.

Surridge, B. W. J., A. J. Baird, and A. L. Heathwaite. "Evaluating the quality of hydraulic conductivity estimates from piezometer slug tests in peat." *Hydrological Processes* 19, no. 6 (2005): 1227-1244.

van Loon, A. H., P. P. Schot, J. Griffioen, M. F. P. Bierkens, O. Batelaan, and M. J. Wassen. "Throughflow as a determining factor for habitat contiguity in a near-natural fen." *Journal of Hydrology* 379 (2009): 30-40.

Weiss, R., J. Alm, R. Laiho, and J. Laine. "Modeling moisture retention in peat soils." *Soil Science Society of America Journal* 62 (1998): 305-315.

Whittington, P. N., and J. S. Price. "The effects of water table draw-down (as a surrogate for climate change) on the hydrology of a fen peatland, Canada." *Hydrological Processes* 20 (2006): 3589-3600.

Wu, J., and N. T. Roulet. "Climate change reduces the capacity of northern peatlands to absorb the atmospheric carbon dioxide: The different responses of bogs and fens." *Global Biogeochemical Cycles* 28, no. 10 (2014): 1005-1024.

APPENDIX A. FIELD DATA

This section contains field data for every infiltration test analyzed as part of this research.

A.1 Large sedge fens

A.1.1 Big Meadows

Table A-1. Big Meadows infiltration test 1.

Time (min)	Interval (min)	Volume added (mL)	Inflow rate (mL/min)	Measurement error (mL/min)
4	4	11800	2950.0	30
7	3	8480	2826.7	33.3
10	3	8000	2666.7	33.3
13	3	8000	2666.7	33.3
16	3	8000	2666.7	33.3
19	3	7820	2606.7	26.7
22	3	7620	2540.0	26.7
25	3	7520	2506.7	26.7
28	3	7840	2613.3	26.7
31	3	7780	2593.3	26.7
34	3	7980	2660.0	26.7
37	3	7310	2436.7	26.7
40	3	7700	2566.7	26.7
43	3	7580	2526.7	26.7

Table A-2. Big Meadows infiltration test 2.

Time (min)	Interval (min)	Volume added (mL)	Inflow rate (mL/min)	Measurement error (mL/min)
3	3	5780	1926.7	20
6	3	5700	1900.0	20
9	3	5590	1863.3	20
12	3	5480	1826.7	20
15	3	5340	1780.0	20
18	3	5200	1733.3	20
21	3	5420	1806.7	20
24	3	5280	1760.0	20
27	3	5260	1753.3	20
30	3	5240	1746.7	20
33	3	5220	1740.0	20
36	3	5180	1726.7	20
39	3	5220	1740.0	20
42	3	5260	1753.3	20
45	3	5200	1733.3	20
48	3	5300	1766.7	20
51	3	5120	1706.7	20

Table A-3. Big Meadows infiltration test 3.

Time (min)	Interval (min)	Volume added (mL)	Inflow rate (mL/min)	Measurement error (mL/min)
3	3	6930	2310.0	26.7
6	3	5850	1950.0	20
9	3	5560	1853.3	20
12	3	5260	1753.3	20
15	3	5200	1733.3	20
18	3	4910	1636.7	20
21	3	4760	1586.7	20
24	3	4850	1616.7	20
27	3	4780	1593.3	20
30	3	4600	1533.3	20
33	3	4640	1546.7	20
36	3	4720	1573.3	20
40	4	5830	1457.5	15
43	3	4720	1573.3	20

Table A-4. Big Meadows infiltration test 4.

Time (min)	Interval (min)	Volume added (mL)	Inflow rate (mL/min)	Error (mL/min)
3	3	9780	3260.0	33.3
6	3	8900	2966.7	33.3
9	3	8000	2666.7	33.3
12	3	8000	2666.7	33.3
15	3	8480	2826.7	33.3
18	3	7320	2440.0	26.7
21	3	7240	2413.3	26.7
24	3	7200	2400.0	26.7
27	3	6900	2300.0	26.7
30	3	6880	2293.3	26.7
33	3	6570	2190.0	26.7
36	3	7200	2400.0	26.7
39	3	7080	2360.0	26.7
42	3	7340	2446.7	26.7
45	3	7200	2400.0	26.7
48	3	7140	2380.0	26.7

Table A-5. Big Meadows infiltration test 5.

Time (min)	Interval (min)	Volume added (mL)	Inflow rate (mL/min)	Measurement error (mL/min)
3	3	9020	3006.7	33.3
6	3	7600	2533.3	26.7
9	3	7040	2346.7	26.7
12	3	6980	2326.7	26.7
15	3	6600	2200	26.7
18	3	5560	1853.3	20
21	3	5540	1846.7	20
24	3	5500	1833.3	20
27	3	5420	1806.7	20
30	3	5300	1766.7	20
33	3	5240	1746.7	20
36	3	5100	1700	20
39	3	5060	1686.7	20
42	3	4700	1566.7	20
45	3	4820	1606.7	20
48	3	4740	1580	20
51	3	4700	1566.7	20
54	3	4580	1526.7	20
57	3	4500	1500	20
60	3	4580	1526.7	20
63	3	4540	1513.3	20

A.1.2 Green Mountain Fen

Table A-6. Green Mountain Fen infiltration test 1.

Time (min)	Interval (min)	Volume added (mL)	Inflow rate (mL/min)	Measurement error (mL/min)
5	5	4000	800	8
10	5	3950	790	8
15	5	3680	736	8
20	5	3640	728	8
25	5	3540	708	8
30	5	3280	656	8
35	5	3320	664	8
40	5	3280	656	8
45	5	3300	660	8

Table A-7. Green Mountain Fen infiltration test 2.

Time (min)	Interval (min)	Volume added (mL)	Inflow rate (mL/min)	Measurement error (mL/min)
5	5	1680	336	4
10	5	1480	296	4
15	5	1440	288	4
20	5	1380	276	4
25	5	1340	268	4
30	5	1340	268	4
35	5	1280	256	4
40	5	1340	268	4
45	5	1240	248	4
50	5	1260	252	4
55	5	1200	240	4
60	5	1240	248	4
65	5	1240	248	4

Table A-8. Green Mountain Fen infiltration test 3.

Time (min)	Interval (min)	Volume added (mL)	Inflow rate (mL/min)	Measurement error (mL/min)
5	5	2650	530	8
10	5	2400	480	8
15	5	2280	456	8
20	5	2200	440	8
25	5	2180	436	8
30	5	2140	428	8
35	5	2000	400	4
40	5	1880	376	4
45	5	1900	380	4
50	5	1840	368	4
55	5	1900	380	4

Table A-9. Green Mountain Fen infiltration test 4.

Time (min)	Interval (min)	Volume added (mL)	Inflow rate (mL/min)	Measurement error (mL/min)
5	5	660	132	4
10	5	760	152	4
15	5	540	108	4
20	5	620	124	4
25	5	550	110	4
30	5	630	126	4
35	5	660	132	4
40	5	720	144	4
45	5	660	132	4
50	5	520	104	4
55	5	540	108	4
60	5	540	108	4
65	5	520	104	4

Table A-10. Green Mountain Fen infiltration test 5.

Time (min)	Interval (min)	Volume added (mL)	Inflow rate (mL/min)	Measurement error (mL/min)
5	5	560	112	4
10	5	500	100	4
15	5	560	112	4
20	5	660	132	4
25	5	370	74	4
30	5	580	116	4
35	5	580	116	4
40	5	600	120	4
45	5	340	68	4
50	5	490	98	4
55	5	460	92	4

Table A-11. Green Mountain Fen infiltration test 6.

Time (min)	Interval (min)	Volume added (mL)	Inflow rate (mL/min)	Measurement error (mL/min)
5	5	4340	868	12
10	5	3920	784	8
15	5	3560	712	8
20	5	3390	678	8
25	5	3390	678	8
30	5	3320	664	8
35	5	3280	656	8
40	5	3330	666	8
45	5	3260	652	8
50	5	3320	664	8

A.2. Small sedge fens

A.2.1 Hells Fen

Table A-12. Hells Fen infiltration test 1.

Time (min)	Interval (min)	Volume added (mL)	Inflow rate (mL/min)	Measurement error (mL/min)
10	10	630	63	1
20	10	340	34	1
30	10	500	50	1
40	10	430	43	1
50	10	550	55	1
60	10	500	50	1
70	10	490	49	1

Table A-13. Hells Fen infiltration test 2.

Time (min)	Interval (min)	Volume added (mL)	Inflow rate (mL/min)	Measurement error (mL/min)
10	10	790	79	1
20	10	800	80	1
30	10	860	86	1
40	10	770	77	1
50	10	750	75	1

Table A-14. Hells Fen infiltration test 3.

Time (min)	Interval (min)	Volume added (mL)	Inflow rate (mL/min)	Measurement error (mL/min)
10	10	1500	150	2
20	10	1290	129	2
30	10	1200	120	2
40	10	1250	125	2
50	10	1250	125	2

Table A-15. Hells Fen infiltration test 4.

Time (min)	Interval (min)	Volume added (mL)	Inflow rate (mL/min)	Measurement error (mL/min)
10	10	580	58	1
20	10	380	38	1
30	10	400	40	1
40	10	525	52.5	1
50	10	480	48	1
60	10	450	45	1

A.2.2 Spring Fen

Table A-16. Spring Fen infiltration test 1.

Time (min)	Interval (min)	Volume added (mL)	Inflow rate (mL/min)	Measurement error (mL/min)
10	10	1430	143	2
20	10	1690	169	2
30	10	1360	136	2
40	10	1590	159	2
50	10	1430	143	2

Table A-17. Spring Fen infiltration test 2.

Time (min)	Interval (min)	Volume added (mL)	Inflow rate (mL/min)	Measurement error (mL/min)
10	10	2280	228	3
20	10	2480	248	3
30	10	2120	212	3
40	10	1970	197	2
50	10	1970	197	2
60	10	1950	195	2

Table A-18. Spring Fen infiltration test 3.

Time (min)	Interval (min)	Volume added (mL)	Inflow rate (mL/min)	Measurement error (mL/min)
10	10	340	34	1
20	10	200	20	1
30	10	260	26	1
40	10	260	26	1
50	10	270	27	1

Table A-19. Spring Fen infiltration test 4.

Time (min)	Interval (min)	Volume added (mL)	Inflow rate (mL/min)	Measurement error (mL/min)
10.5	10.5	950	90.5	1
20	9.5	890	93.7	1
30	10	910	91	1
40	10	860	86	1
50	10	875	87.5	1
60	10	890	89	1

A.3 Heterogeneous fens

A.3.1 Sphagnum Fen

Table A-20. Sphagnum Fen infiltration test 1.

Time (min)	Interval (min)	Volume added (mL)	Inflow rate (mL/min)	Measurement error (mL/min)
3	3	8000	2666.7	26.7
6	3	7675	2558.3	26.7
9	3	6000	2000	20
12	3	7500	2500	26.7
15	3	7025	2341.7	26.7
18	3	6910	2303.3	26.7
21	3	6000	2000	20
24	3	6000	2000	20
27	3	5400	1800	20
30	3	6000	2000	20
33	3	6990	2330	26.7
36	3	5900	1966.7	20
39	3	7400	2466.7	26.7
42	3	5800	1933.3	20
45	3	5820	1940	20
48	3	5820	1940	20

Table A-21. Sphagnum Fen infiltration test 2.

Time (min)	Interval (min)	Volume added (mL)	Inflow rate (mL/min)	Measurement error (mL/min)
3	3	4000	1333.3	13.3
6	3	3860	1286.7	13.3
9	3	3540	1180.0	13.3
12	3	3420	1140.0	13.3
15	3	3320	1106.7	13.3
18	3	3260	1086.7	13.3
21	3	3200	1066.7	13.3
24.5	3.5	3500	1000.0	11.4
27	2.5	2540	1016.0	16.0
30	3	3140	1046.7	13.3
33	3	2850	950.0	13.3
36	3	2820	940.0	13.3
39	3	2760	920.0	13.3
42	3	2860	953.3	13.3
45	3	2780	926.7	13.3
48	3	2900	966.7	13.3
51	3	2760	920.0	13.3

Table A-22. Sphagnum Fen infiltration test 3.

Time (min)	Interval (min)	Volume added (mL)	Inflow rate (mL/min)	Measurement error (mL/min)
3	3	3740	1246.7	13.3
6	3	3420	1140.0	13.3
9	3	3310	1103.3	13.3
12	3	3420	1140.0	13.3
15	3	3000	1000.0	13.3
18	3	3160	1053.3	13.3
21	3	2840	946.7	13.3
24	3	2880	960.0	13.3
27	3	2840	946.7	13.3
30	3	2810	936.7	13.3
33	3	2740	913.3	13.3
36	3	2860	953.3	13.3
39	3	2580	860.0	13.3
42	3	2420	806.7	13.3
45	3	2680	893.3	13.3
48	3	2670	890.0	13.3

Table A-23. Sphagnum Fen infiltration test 4.

Time (min)	Interval (min)	Volume added (mL)	Inflow rate (mL/min)	Measurement error (mL/min)
3	3	1360	453.3	6.7
6	3	1420	473.3	6.7
9	3	1310	436.7	6.7
12	3	1280	426.7	6.7
15	3	1440	480.0	6.7
18	3	1300	433.3	6.7
21	3	1470	490.0	6.7
24	3	1290	430.0	6.7
27	3	1510	503.3	6.7
30	3	1340	446.7	6.7

A.3.2 Circle Fen

Table A-24. Circle Fen infiltration test 1.

Time (min)	Interval (min)	Volume added (mL)	Inflow rate (mL/min)	Measurement error (mL/min)
5	5	4000	800	8.0
10	5	3610	722	8.0
15	5	3170	634	8.0
20	5	3010	602	8.0
25	5	3010	602	8.0
30	5	2720	544	8.0
35	5	2620	524	8.0
40	5	2480	496	8.0
45	5	2360	472	8.0
50	5	2420	484	8.0
55	5	2280	456	8.0

Table A-25. Circle Fen infiltration test 2.

Time (min)	Interval (min)	Volume added (mL)	Inflow rate (mL/min)	Error (mL/min)
5	5	4340	868	12.0
10	5	4000	800	8.0
15	5	3920	784	8.0
20	5	3480	696	8.0
25	5	3600	720	8.0
30	5	3300	660	8.0
35	5	3220	644	8.0
40	5	3220	644	8.0
45	5	3020	604	8.0
50	5	2800	560	8.0
55	5	2880	576	8.0
60	5	2720	544	8.0

Table A-26. Circle Fen infiltration test 3.

Time (min)	Interval (min)	Volume added (mL)	Inflow rate (mL/min)	Measurement error (mL/min)
3	3	8790	2930.0	33.3
6	3	7500	2500.0	26.7
9	3	7540	2513.3	26.7
12	3	7300	2433.3	26.7
15.5	3.5	7875	2250.0	22.9
18	2.5	5900	2360.0	24.0
21	3	6450	2150.0	26.7
24	3	7220	2406.7	26.7
27	3	6700	2233.3	26.7
30	3	6000	2000.0	20.0

Table A-27. Circle Fen infiltration test 4.

Time (min)	Interval (min)	Volume added (mL)	Inflow rate (mL/min)	Measurement error (mL/min)
5	5	2640	528	8.0
10	5	2480	496	8.0
15	5	2420	484	8.0
20	5	2430	486	8.0
25	5	2460	492	8.0
30	5	2420	484	8.0

Table A-28. Circle Fen infiltration test 5.

Time (min)	Interval (min)	Volume added (mL)	Inflow rate (mL/min)	Measurement error (mL/min)
6	6	6560	1093.3	13.3
10	4	3620	905	10
15	5	4660	932	12
20	5	4400	880	12
25	5	4000	800	8
30	5	4000	800	8
35	5	3460	692	8
40	5	3620	724	8